

Theoretical Investigation of the Input Impedance of Gap-Coupled Circular Microstrip Patch Antennas

Pradeep Kumar · Ghanshyam Singh

Received: 5 February 2009 / Accepted: 15 June 2009 /
Published online: 14 July 2009
© Springer Science + Business Media, LLC 2009

Abstract In this paper, we have explored a simple theoretical input impedance computation technique for the two gap-coupled circular microstrip patch antennas by using circuit theory approach. The frequency characteristics of the input impedance of the two gap-coupled circular microstrip patch antennas with the gap-distance between the feed patch and parasitic patch is analyzed and simulated. The effect of feed location in the feed patch on the input impedance of proposed antenna is also studied. The theoretical results are compared with the simulated results as well as other reported literature. The simulation has been performed by using a method-of-moment based commercially available simulator IE3D.

Keywords Microstrip antenna · Gap-coupling · Bandwidth · Efficiency · Gain · Circuit model

1 Introduction

Microstrip patch antennas are used in the wide range of applications such as aircraft, satellite, missiles, land vehicles and in small portable wireless communication equipments due to their compactness, light weight, low-profile, and relative ease of fabrication method [1]. To a large extent, the development of microstrip antennas has been driven by systems requirements. The disadvantages of the microstrip patch antenna configurations include narrow impedance bandwidth, spurious feed radiation, poor polarization purity, limited power capacity and tolerance problems which limits their more widespread applications. The impedance bandwidth and input impedance are the potential properties of the microstrip patch antenna that is strongly affected by the substrate thickness. The impedance bandwidth of the microstrip antenna can be increased using various techniques such as by loading a patch, by using a thicker substrate and by reducing the dielectric constant.

P. Kumar · G. Singh (✉)
Department of Electronics and Communication Engineering,
Jaypee University of Information Technology, Solan 173 215, India
e-mail: drghanshyam.singh@yahoo.com

However, limitations still exist on the ability to effectively feed the patch on thicker substrate and radiation efficiency which degrades with increasing the substrate thickness causes generation of spurious radiation [1].

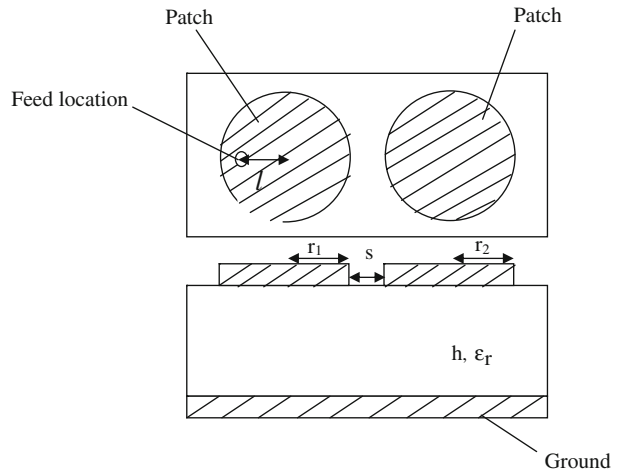
Recently, more progress has been made to increase the impedance bandwidth of the microstrip patch antennas [1–3]. Pozar [1] listed the impedance bandwidths for the microstrip patch antennas with several shapes such as rectangular, square, and circular with different feeding techniques. The potential techniques to enhance the impedance bandwidth of microstrip patch antennas are parasitic elements [4–11], aperture coupled [12, 13], and impedance matching network [14]. A broad-band matching design procedure with external matching has been presented in [15] to improve the bandwidth characteristics of several microstrip patch antennas. Among various antenna bandwidth enhancement configuration techniques, the two gap-coupled circular microstrip patch antenna is most significant. In the configuration of gap-coupled microstrip antennas, two patches are placed close to each other. The gap-coupled microstrip antennas generate two resonant frequencies and the bandwidth of the microstrip antennas can be increased by the proper adjustment of feeding and dimensions. There are two potential advantages of the gap-coupled circular microstrip antennas over conventional circular microstrip antennas: 1) bandwidth can be enhanced, and 2) it can be used for dual frequency applications. Ray *et al* [16] have designed dual and triple frequency band operation gap-coupled microstrip patch antenna. Ansari *et al* [17] have also presented the analysis of the gap-coupled stacked annular ring microstrip antenna.

In this paper, the concept of coupled microstrip lines [18] is extended for the two gap-coupled circular microstrip patch antennas to analyze the input impedance by using circuit theory approach and the results are compared with the simulated results. The effects of mutual coupling between the radiating apertures have been taken into account. The exact computation of the input impedance of the proposed antenna is used to match the impedance for enhance the impedance bandwidth [14]. In the analysis, total capacitance of microstrip patch antenna is taken as parallel plate capacitance and two fringing capacitances for both even and odd modes. Since there is another patch that is parasitic element in the proposed two gap-coupled circular microstrip patch antennas, so there is another fringing capacitance at the adjacent edge of the patches. This effort has involved for the design of novel microstrip antenna configurations, and development of accurate and versatile models for understanding of the inherent limitations of microstrip antennas as well as for their design and optimization. The organization of the paper is as follows. The Section 2 is concerned with the geometrical configuration of the two gap-coupled circular microstrip patch antennas. The Section 3 discusses about the theoretical formulation of the proposed antenna. The simulation and analytical results have been discussed in Section 4, and finally Section 5 concludes the work.

2 Antenna configuration

The geometrical configuration of two gap-coupled circular microstrip antennas is shown in Fig. 1. The patch of radius $r_1=15$ mm is the feed patch and other patch of radius $r_2=15$ mm is the parasitic patch. The parasitic patch is excited by the gap-coupling whereas the feed patch is excited by the coaxially probe feeding technique. The location of coaxial probe is at distance $l=4$ mm, from the center of the patch as shown in Fig. 1. The microstrip patch antenna, generally, used either microstrip line or coaxially probe feed technique. These two feeding techniques are very similar in operation, and offer essentially one degree of freedom in the design of antenna element through the positioning of the feed point to adjust

Fig. 1 Geometrical configurations of the two gap-coupled circular microstrip patch antennas.



the input impedance level. The coaxially fed microstrip antennas have two key exciting sources, namely, the probe electric current and the coaxial electric field. In the calculation of the input impedance of probe-driven microstrip antennas on thin substrates, the effects of the probe results in an additional inductive component to the input impedance. The probe inductance has been accounted by several authors through use of a simple formula [19–22]. The parasitic patch introduces another resonance near the main resonance and proper adjustment of the structure parameters, bandwidth can be enhanced. The height and relative permittivity of the substrate is $h=1.59$ mm and $\epsilon_r=2.2$, respectively. The gap distance between the adjacent edges of the feed patch and parasitic patch is s .

3 Formulation

The coupled microstrip structures can be characterized for the two modes which are known as odd and even modes [18, 23]. The properties of coupled microstrip patches have been determined by the self and mutual inductance and capacitance between the patches. Under the quasi-transverse electromagnetic mode approximation the self-inductance can be expressed in term of self-capacitance by using simple relations. For most of the practical circuits using symmetric microstrip patches the mutual-inductance and mutual-capacitance are interrelated to each other so it is not necessary to determine each separately. Therefore, only capacitance parameters are evaluated for the two gap-coupled circular microstrip patch antennas. The capacitances can be expressed in terms of even and odd modes values for propagation [18].

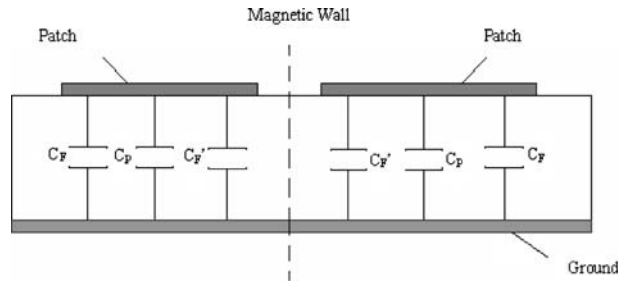
The total capacitance of the coupled structure can be determined by using Figs. 2 and 3 for even mode and odd modes, respectively. From Fig. 2 the total capacitance for even mode, C_E is given by [18]:

$$C_E = C_P + C_F + C_{F'} \quad (1)$$

where C_P is the parallel plate capacitance between metallic patch and the ground plane and is given by:

$$C_P = \frac{\epsilon_0 \epsilon_r A}{h} \quad (2)$$

Fig. 2 Even-mode capacitances of the two gap-coupled circular microstrips patch antennas.



where A is the surface area of the patch and ϵ_r is the relative dielectric permittivity of the substrate and ϵ_0 is the permittivity of free-space. C_F is the fringing capacitance due to edge conductor and given by:

$$C_F = \frac{1}{2} \left[\frac{\sqrt{\epsilon_{eff}}}{cZ_C} - C_P \right] \tag{3}$$

where $c = 3 \times 10^8$ m/s that is velocity of light in vacuum, Z_C is the characteristic impedance and ϵ_{eff} is the effective dielectric permittivity of the substrate. $C_{F'}$ is the fringing capacitance due to parasitic patch and given by:

$$C_{F'} = \frac{C_F}{1 + A \left(\frac{h}{s}\right) \tanh\left(\frac{10s}{h}\right)} \sqrt{\frac{\epsilon_r}{\epsilon_{eff}}} \tag{4}$$

where $A = \exp(-0.1 \exp(2.33 - \frac{2.53C}{2h}))$ and C is the circumference of the patch. With the help of equations (1) to (4), the even mode-capacitance of the two gap-coupled circular microstrip patch antennas is calculated.

From Fig. 3, the total capacitance for odd- mode, C_O is given by [18]:

$$C_O = C_P + C_F + C_{gd} + C_{ga} \tag{5}$$

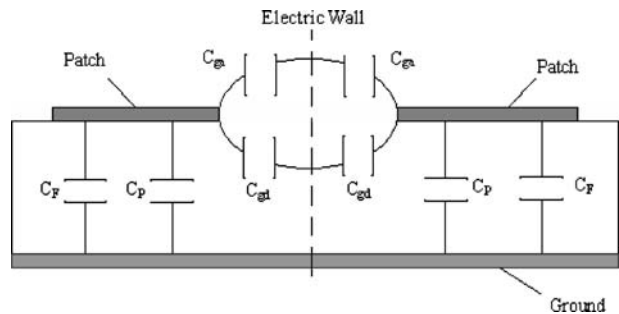
where C_{gd} is the capacitance between two structures through dielectric region and given by:

$$C_{gd} = \frac{\epsilon}{\pi} \ln\left(\coth\left(\frac{\pi s}{4h}\right)\right) + 0.65C_F \left(\frac{0.02\sqrt{\epsilon_r}}{s/h} + 1 - \frac{1}{\epsilon_r^2}\right) \tag{6}$$

and C_{ga} is the capacitance between the structures through air and given by:

$$C_{ga} = \frac{K(k')\epsilon_0}{2K(k)} \tag{7}$$

Fig. 3 Odd-mode capacitances of the two gap-coupled circular microstrip patch antennas.



where $K(k)$, $K(k')$ are elliptic functions, k and k' are:

$$k = \frac{s/h}{s/h + 2(C/h)} \text{ and } k' = \sqrt{1 - k^2}$$

The approach of coupled microstrip line presented in [18] is applied to the two gap-coupled circular microstrip patch antennas. With the help of equation (1)–(7), the capacitances of the two gap-coupled circular microstrip patch antennas for odd and even modes are calculated and compared with the coupled microstrip lines as in [18]. For this comparison the cross-sectional area of the coupled circular microstrip patches and coupled microstrip lines are considered same. In the present results of Table 1, the height of the substrate is taken unity. The even and odd mode capacitances of the coupled circular microstrip patches and coupled microstrip lines are shown in Table 1.

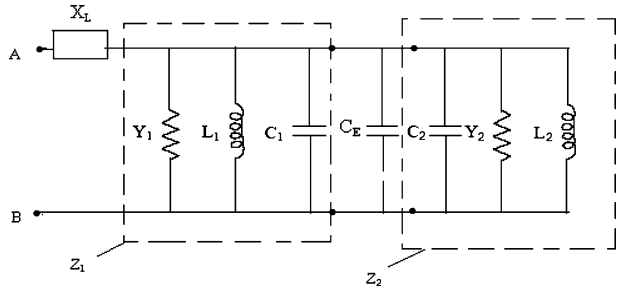
The equivalent circuit model of the two gap-coupled circular microstrip patch antennas for even mode is shown in Fig. 4. From Fig. 4, the input impedance for even mode is calculated. Z_1 and Z_2 are the impedances of feed path and parasitic patch, respectively and given as [24].

$$Z_1 = Z_2 = \frac{R}{1 + Q_T^2 \left(\frac{f}{f_r} - \frac{f_r}{f}\right)^2} + jRQ_T \frac{\left(\frac{f}{f_r} - \frac{f_r}{f}\right)}{1 + Q_T^2 \left(\frac{f}{f_r} - \frac{f_r}{f}\right)^2} \tag{8}$$

Table 1 Comparison of coupled microstrip lines by Garg [18] and our approach to coupled microstrip antennas. ($\epsilon_r=9.7$).

Coupled microstrip lines [18] (L=1)				Proposed approach for gap coupled circular microstrip antennas			
w/h	s/h	C _E (pF)	C _O (pF)	r1/h	s/h	C _E (pF)	C _O (pF)
0.2	0.05	60.3	215	0.253	0.05	57.99	222.3
0.2	0.20	66.1	149	0.253	0.20	62.3	155.2
0.2	0.50	75.7	117	0.253	0.50	70.41	122.5
0.2	1.00	83.5	98.5	0.253	1.00	78.28	102.8
0.2	2.00	89.9	87.2	0.253	2.00	85.8	90.58
0.5	0.05	90.1	258	0.399	0.05	87.9	260.7
0.5	0.20	95.4	188	0.399	0.20	92.3	190.9
0.5	0.50	105	155	0.399	0.50	100.8	157.5
0.5	1.00	114	136	0.399	1.00	109.3	137.4
0.5	2.00	122	124	0.399	2.00	117.6	124.7
1.0	0.05	136	313	0.564	0.05	133	311
1.0	0.20	141	241	0.564	0.20	137.4	239.7
1.0	0.50	150	207	0.564	0.50	146	206
1.0	1.00	159	187	0.564	1.00	154.7	185.5
1.0	2.00	168	174	0.564	2.00	163.4	172.6
2.0	0.05	223	408	0.798	0.05	220.3	402.1
2.0	0.20	228	334	0.798	0.20	224.6	330.1
2.0	0.50	237	300	0.798	0.50	233.2	295.9
2.0	1.00	246	279	0.798	1.00	241.9	275.3
2.0	2.00	255	266	0.798	2.00	250.5	262.2

Fig. 4 An equivalent circuit model of the two gap-coupled circular microstrip antennas for the even mode.



where R is the resonant resistance of the resonant parallel RLC circuit, f_r is the resonant frequency and Q_T is quality factor associated with system loss including radiation from the walls (Q_R), losses in dielectric (Q_D), and losses in conductor (Q_C). Q_T can be calculated by [24, 25]:

$$Q_T = \frac{1}{\frac{1}{Q_R} + \frac{1}{Q_C} + \frac{1}{Q_D}} \tag{9}$$

$$Q_R = \frac{4\pi(\alpha^2 - 1)\epsilon_r^{3/2}}{h\alpha^3 F(\alpha/\sqrt{\epsilon_r})} \tag{10}$$

where

$$F(x) = \frac{4}{x^3} \left\{ 2xJ_0(2x) + (x^2 - 1) \int_0^{2x} J_0(t)dt \right\} \tag{11}$$

$$F(x) = 2.666667378 - 1.066662519x^2 + 0.209534311x^4 - 0.019411347x^6 + 0.001044121x^8 - 0.000049747x^{10} \tag{12}$$

$$Q_D = \frac{1}{\tan \delta} \tag{13}$$

where $\tan \delta$ is dielectric loss tangent and α is the n^{th} zero of first derivative of Bessel function of first order.

$$Q_C = \frac{h}{\delta_s} \tag{14}$$

where δ_s is the skin depth and given by:

$$\delta_s = \frac{1}{\sqrt{\pi f \mu_0 \sigma}} \tag{15}$$

$$R = \frac{1}{G_T} \frac{J_1^2(k.l)}{J_1^2(kr_1)} \tag{16}$$

where G_T includes the conductance due to ohmic, dielectric and radiation losses, and l is the distance of feed point from the center.

$$G_T = G_R + G_D + G_C \quad (17)$$

where

$$G_R = \frac{2.39}{4\mu_0 f_r h Q_R} \quad (18)$$

$$G_D = \frac{2.39 \tan \delta}{4\mu_0 f_r h} \quad (19)$$

$$G_C = \frac{2.39\pi(\pi f_r \mu_0)^{-3/2}}{4h^2 \sqrt{\sigma}} \quad (20)$$

$$J_1(t) = t(0.5 - 0.56249985\left(\frac{t}{3}\right)^2 + 0.21093573\left(\frac{t}{3}\right)^4 - 0.03954289\left(\frac{t}{3}\right)^6 + 0.00443319\left(\frac{t}{3}\right)^8 - 0.0031761\left(\frac{t}{3}\right)^{10}) \quad (21)$$

X_L is the inductance due to probe feeding and given by [24]:

$$X_L = j \frac{3.77fh}{c} \log\left(\frac{c}{\pi f d_0}\right) \quad (22)$$

where d_0 is the diameter of the coaxial feed probe. The conductance, inductance and the capacitance in the Figs. 4 and 5 are given by [26]:

$$Y_1 = Y_2 = \frac{1}{R} \quad (23)$$

$$L_1 = L_2 = \frac{R}{2\pi f_r Q_T} \quad (24)$$

$$C_1 = C_2 = \frac{Q_T}{2\pi f_r R} \quad (25)$$

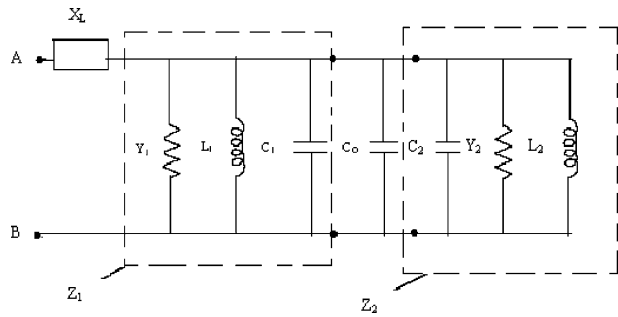
An equivalent circuit model of the two gap-coupled circular microstrip antennas for the odd mode is given in Fig. 5. From Fig. 5, the input impedance for the odd mode is calculated.

The total input impedance of the gap-coupled structures is given by [23]:

$$Z_{in} = Z_{in}^E + Z_{in}^O \quad (26)$$

where Z_{in}^E and Z_{in}^O are the input impedance for the even and odd mode, respectively. Using aforementioned equations, we can calculate the input impedance of the two gap-coupled

Fig. 5 An equivalent circuit model of the two gap-coupled circular microstrip patch antennas for the odd mode.



circular microstrip patch antennas. The gap capacitance between two structures through dielectric (C_{gd}) is directly proportional to the fringe capacitance that is increases with increasing the fringe capacitance and decreases with decreasing the fringe capacitance as from Equation (6). While the gap capacitance between two structures through air (C_{ga}) is independent from the fringing capacitance as from Equation (7). Both the gap capacitances that is gap capacitance between two structures through dielectric (C_{gd}) and through air (C_{ga}) depends upon the gap between adjacent edges of the feed patch and parasitic patch. The variation of these capacitances with gap distance is shown in Table 2. From Table 2, it is clear that both gap capacitances decrease with increasing the gap.

4 Results and discussion

The input impedance is defined as the ratio of voltage across the patch and ground plane to the feed point current. The numerical results for the input impedances calculated without the inclusion of the coaxial aperture field, only the probe electric current is considered because the coaxial aperture field is negligible at lower frequencies whereas at higher frequencies the effect is large. The probe current is assumed to have only an axially directed unit electric line current with no angular variations. This assumption is reasonable since the substrate thickness is small compared to the wavelength [27]. The input impedance of the two gap-coupled circular microstrip patch antenna is calculated by using (26) and the computed results are compared with simulated results. The simulation of the proposed antenna is performed by a commercially available method-of-moment based simulator IE3D. In the numerical computation and simulation of the proposed antenna the location of coaxial probe feed is at $l=4$ mm away from the center of the feed patch as shown in Fig. 1.

The frequency characteristics of the input impedance (real and imaginary part) of two gap-coupled circular microstrip patch antennas are shown in Fig. 6. With the increase of

Table 2 Variation of gap capacitances with gap distance between adjacent edges of feed patch and parasitic patch ($r_1=r_2=15$ mm, $\epsilon_r=2.2$, $h=1.59$ mm).

Gap distance s (mm)	C_{ga} (pF)	C_{gd} (pF)
0.1	46.4	28.64
0.5	37.37	15.8
1	33.5	11.48
2	29.65	8.178
4	25.86	6.593

frequency, the real part of input impedance increases and attain an optimum value at a particular frequency (3.77 GHz) and then start to decrease, whereas the imaginary part of the input impedance almost always decreases as shown in Fig. 6. The comparison of simulated and computed results shows good agreement in a range of frequencies. Initially, in a short range of frequency the simulated and computed results are differing. In an earlier reported literature [6], it has been shown that the gap-coupling lead to close resonance of the TM_{11} and TM_{21} mode. Here, we have computed the frequency characteristics of the input impedance only for TM_{21} mode, however, the deviation seen in Fig. 6 for initial frequencies is due to presence of the TM_{11} mode in simulation results.

The variation of the real and imaginary part of the input impedance of the proposed antenna with gap distance between adjacent edges of the patch is shown in Fig. 7. The computed and simulated results in the particular range of the gap distance between the feed patch and parasitic patch of the proposed antenna are well matched.

Further, the variation of real and imaginary part of the input impedance with feed location from center of the patch is shown in Fig. 8. From Fig. 8, it is clear that the both real and imaginary part of the input impedance of the proposed antenna increases when the feeding probe moves from center towards the edge of the patch. In terms of the transmission line model, the antenna is viewed as a length open circuited transmission line with light loading at the end to account for fringing fields and radiations. The voltage and current on this equivalent transmission line give the input impedance variation of the microstrip antenna. For a feed point at a radiating edge, the voltage is maximum and current is minimum so the input impedance is maximum. For a feed point at the center of patch, the voltage is zero and current is maximum, so the input impedance is zero. Thus the input impedance can be controlled by adjusting the position of feed point. The simulated field pattern of the proposed antenna at 3.77 GHz for E-plane and H-plane is shown in Fig. 9 (a) and (b), respectively.

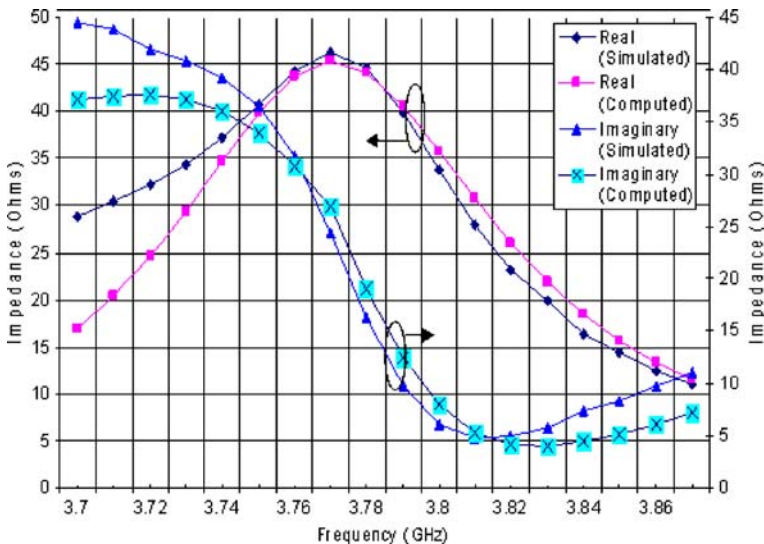


Fig. 6 Frequency characteristics of the input impedance of the two gap-coupled circular microstrip patch antennas for the gap distance between the feed patch and parasitic patch is 1.5 mm.

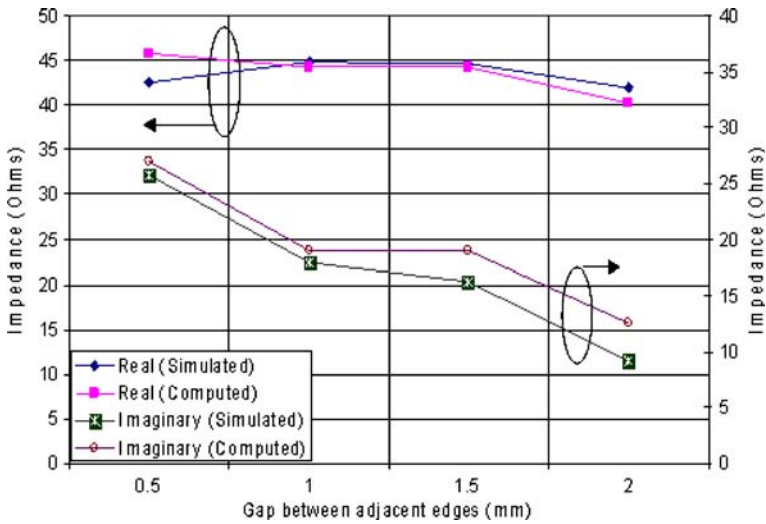


Fig. 7 The gap distance characteristics of input impedance of the two gap-coupled circular microstrip patch antenna with gap between adjacent edges of the feed patch and parasitic patch at frequency 3.78 GHz.

5 Conclusion

A simple and numerically efficient model for the input impedance of two gap-coupled circular microstrip patch antennas is developed. Input impedance for different gap distances between adjacent edges of feed patch and parasitic patch is shown as well as the variation of input impedance with feed location is also discussed. The input impedance depends heavily on the feed location and increases when feed point moves from center towards edge

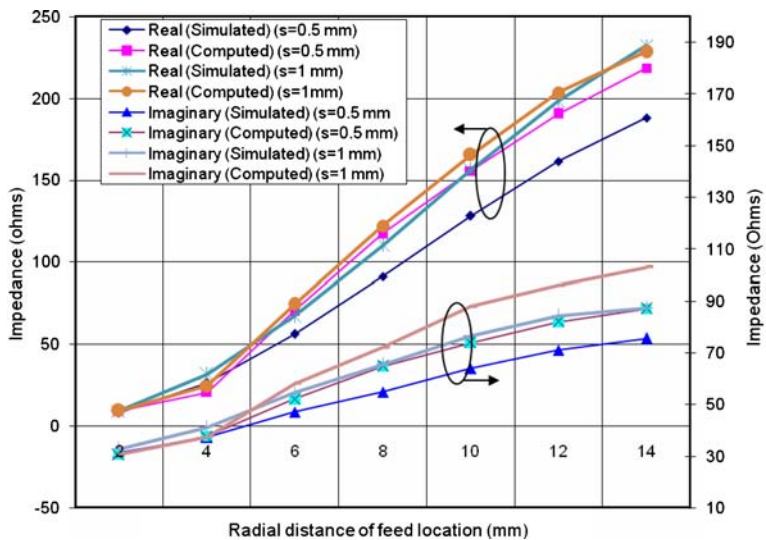
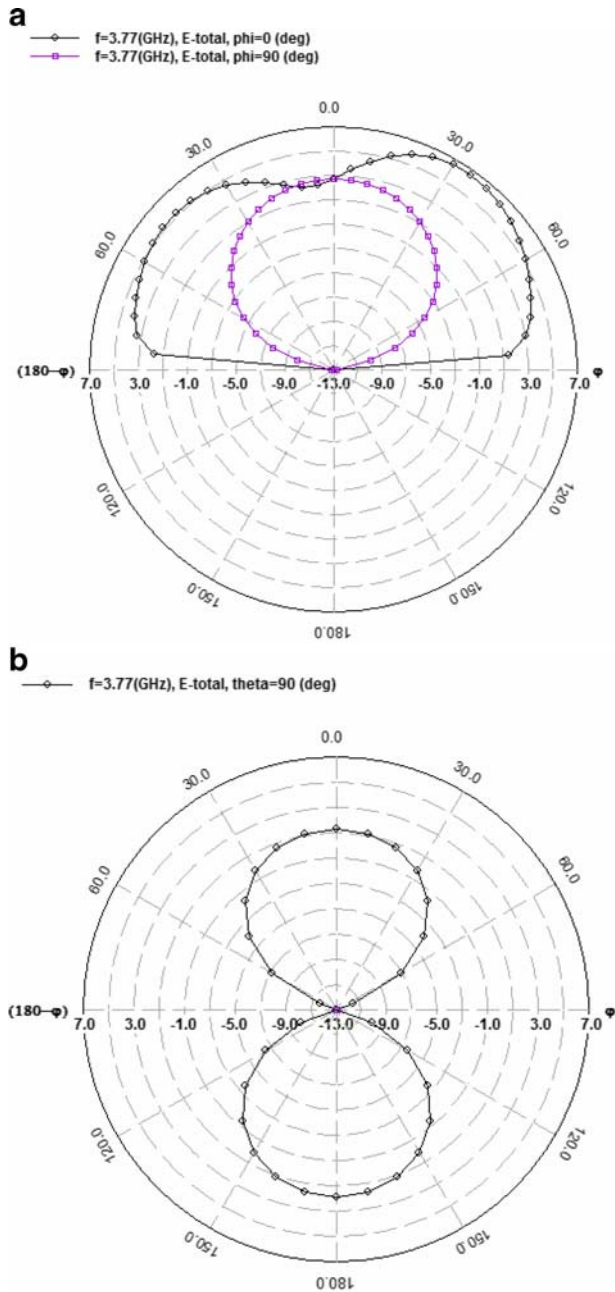


Fig. 8 Feed location characteristics of the input impedance of the two gap-coupled circular microstrip patch antenna at 3.72 GHz for different gap distance between adjacent edges of the feed patch and parasitic patch.

Fig. 9 Simulated radiation pattern at 3.77 GHz, (a) E-plane, (b) H-plane.



of the patch. The comparison between the analytical and simulated results shows good agreement. An asymmetric gap-coupled microstrip antenna configuration has an inherent capability for impedance transformation which can be used for tapered antenna arrays that will be reported in future communications.

Acknowledgment Authors are sincerely thankful to the reviewer for critical comments and suggestions to improve the quality of the manuscript.

References

1. D. M. Pozar and D. H. Schaubert, *Microstrip Antennas* (IEEE Press, New York, 1995).
2. M. Albooyeh, N. Kamjani, and M. Shobeyri, “A novel cross-slot geometry to improve impedance bandwidth of microstrip antennas,” *Progress In Electromagnetics Research Letters* **4**, 63–72 (2008).
3. S. S. Yang, K.-F. Lee, A. A. Kishk, and K.-M. Luk, “Design and study of wideband single feed circularly polarized microstrip antennas,” *Progress In Electromagnetics Research*, *PIER* **80**, 45–61 (2008).
4. Surrakanth Nirate, Ravi M. Yadahalli, Usha Kiran K, Vani R. M, and P. V. Hunagund, “Wideband gap-coupled suspended rectangular microstrip antenna,” *Proceedings of Int. Conf. on Recent Advances in Microwave and Applications (Microwave-08)*, pp. 833–835, Jaipur, India, 2008.
5. Ramesh Garg and V. S. Reddy, “A broad-band coupled-strips microstrip antenna,” *IEEE Transactions on Antennas and Propagation* **49** (9), 1344–1345 (2001).
6. R. Kapur and G. Kumar, “Hybrid-coupled shorted rectangular microstrip antennas,” *Electronics Letters* **35** (18), 1501–1502 (1999).
7. K. R. Carver and J. W. Mink, “Microstrip antenna technology,” *IEEE Transactions on Antennas and Propagation* **29**, 2–24 (1981).
8. G. Kumar and K. C. Gupta, “Non-radiating edges and four-edge gap coupled with multiple resonator, broadband microstrip antennas,” *IEEE Transactions on Antennas and Propagation* **33**, 173–178 (1985).
9. P. Kumar, T. Chakravarty, G. Singh, S. Bhooshan, A. De, and S. K. Khah, “Numerical computation of resonant frequency of gap-coupled microstrip antennas,” *Journal of Electromagnetic Waves and Applications* **21** (10), 1303–1311 (2007).
10. P. Kumar and G. Singh, “Computation of mutual coupling of gap-coupled circular patch antenna loaded with shorting post,” *International Journal of Electronic Engineering* **1** (1), 99–102 (2009).
11. K. Araki, H. Ueda, and M. Takahashi, “Numerical analysis of circular disk microstrip antenna with parasitic elements,” *IEEE Transactions on Antennas and Propagation* **34** (12), 1390–1394 (1986).
12. I. Park and R. Mittra, “Aperture-coupled small microstrip antenna,” *Electronics Letters* **32** (19), 1741–1741 (1996).
13. S. D. Targonski and R. B. Waterhouse, “and Pozar, “Wideband aperture coupled stacked patch antenna using thick substrates,”” *Electronics Letters* **32** (21), 1941–1942 (1996).
14. A. Hongming, B. K. J. C. Nauwelaers, and A. R. Van de Capelle, “Broadband active microstrip antenna design with the simplified real frequency technique,” *IEEE Transactions on Antennas and Propagation* **42**, 1612–1619 (1994).
15. H. F. Pues and A. R. Van de Capelle, “An impedance-matching technique for increasing the bandwidth of microstrip antennas,” *IEEE Transactions on Antennas and Propagation* **37**, 1345–1354 (1989).
16. K. P. Ray, V. Sevani, and R. K. Kulkarni, “Gap coupled rectangular microstrip antennas for dual and triple frequency operation,” *Microwave and Optical Technology Letter* **49** (6), 1480–1486 (2007).
17. J. A. Ansari, R. B. Ram, and P. Singh, “Analysis of a gap-coupled stacked annular ring microstrip antenna,” *Progress In Electromagnetics Research B* **4**, 147–158 (2008).
18. R. Garg, “Design equations for coupled microstrip lines,” *International Journal of Electronics* **47** (6), 587–591 (1979).
19. D. M. Pozar, “Input impedance and mutual coupling of rectangular microstrip antenna,” *IEEE Transactions on Antennas and Propagation* **23**, 1191–1196 (1982).
20. W. C. Chew and J. A. Kong, “Analysis of a circular microstrip disk antenna with a thick dielectric substrate,” *IEEE Transactions on Antennas and Propagation* **29**, 68–73 (1981).
21. M. Davidovitz and Y. T. Lo, “Input impedance of a probe fed circular microstrip antenna with thick substrate,” *IEEE Transactions on Antennas and Propagation* **34**, 905–911 (1986).
22. A. N. Tulintseff, S. M. Ali, and J. A. Kong, “Input impedance of a probe fed stacked circular microstrip antenna,” *IEEE Transactions on Antennas and Propagation* **39**, 381–390 (1991).
23. Minh-Chau T. Huyngh, “A numerical and experimental investigation of planar inverted-F antennas for wireless communication applications”, MS Thesis, Virginia Polytechnic Institute and State University, Blacksburg, Virginia, 2000.

24. F. Abboud, J. P. Damiano, and A. Papiernik, “A new model for calculating the input impedance of coax-fed circular microstrip antennas with and without air gaps,” *IEEE Transactions on Antennas and Propagation* **38** (11), 1882–1885 (1990).
25. R. Garg, P. Bhartiya, I. Bahl, and A. Ittipiboon, *Microstrip Antenna Design Handbook* (Artech House Publishers, London, 2001).
26. I. J. Bahal and P. Bhartiya, *Microstrip Antenna* (Artech House, Boston, MA, 1988).
27. C.-H. Huang and P. Hsu, “Effects of feed modeling on the evaluation of input impedance of microstrip antennas,” *IEEE Transactions on Magnetics* **25** (4), 3058–3060 (1989).